AD-A080 222 NAVAL UNDERWATER SYSTEMS CENTER NEW LONDON CT NEW LO--ETC F/G 20/1
TRANSMISSION LOSS THROUGH CASCADED GRATINGS OF SIMPLY SUPPORTED--ETC(U)
DEC 79 R P RADLINSKI, F E REMBETSKI

UNCLASSIFIED NUSC-TR-6117 NL

| OF |
AD A080222

END
DATE FILMED
3-80
DDC

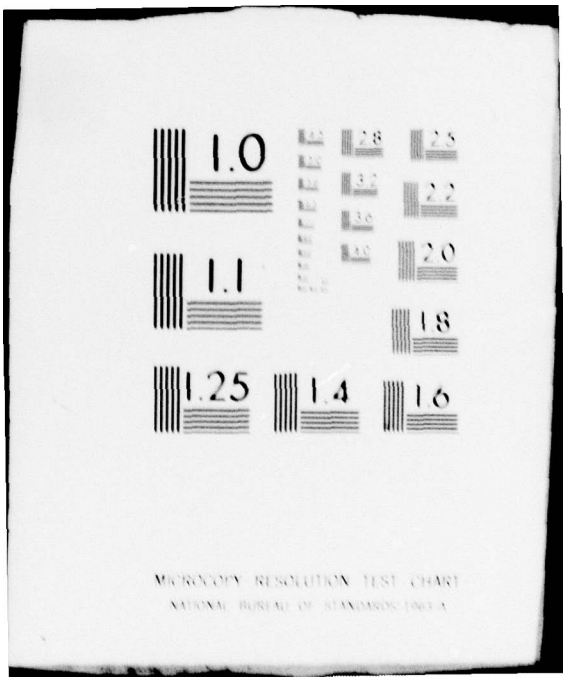
1.0
1.1
1.25
1.4
1.6
2.8
3.2
3.6
4.0
2.5
2.2
2.0
1.8
MICROCOPY RESOLUTION TEST CHART
NATIONAL BUREAU OF STANDARDS-1963-A

NUSC Technical Report 6117

NUSC Technical Report 6117

Transmission Loss Through Cascaded Gratings of Simply Supported Hollow Bars In a Fluid Layer

Ronald P. Radlinski
Francis E. Rembetski
Special Projects Department

19 December 1979

NUSC
Naval Underwater Systems Center
Newport, Rhode Island • New London, Connecticut

Preface

This project was done under NUSC Project No. A70008, "Compliant Tube Development," Principal Investigator, Dr. R. P. Radlinski (Code 313), and Navy Subproject No. S0221-AS, Program Manager, Robert A. Rippeon, David Taylor Naval Ship Research and Development Center (Code 1905).

The Technical Reviewer for this report was Dr. C. H. Sherman, Code 316.

Reviewed and Approved: 19 December 1979

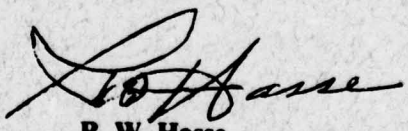

R. W. Hasse
Head: Special Projects Department

The authors of this report are located at the New London Laboratory, Naval Underwater Systems Center, New London, Connecticut 06320.

(14) NUSC-TR-6117

REPORT DOCUMENTATION PAGE

READ INSTRUCTIONS BEFORE COMPLETING FORM

1. REPORT NUMBER: TR 6117	2. GOVT ACCESSION NO.
3. RECIPIENT'S CATALOG NUMBER	
4. TITLE (and Subtitle): (6) TRANSMISSION LOSS THROUGH CASCADED GRATINGS OF SIMPLY SUPPORTED HOLLOW BARS IN A FLUID LAYER	5. TYPE OF REPORT & PERIOD COVERED
	6. PERFORMING ORG. REPORT NUMBER
7. AUTHOR(s): (10) Ronald P. Radlinski, Francis E. Rembetski	8. CONTRACT OR GRANT NUMBER(s): (9) Technical rept.
9. PERFORMING ORGANIZATION NAME AND ADDRESS: Naval Underwater Systems Center, New London Laboratory, New London, CT 06320	10. PROGRAM ELEMENT, PROJECT, TASK AREA & WORK UNIT NUMBERS: A70008, S0221-AS (12) 26
11. CONTROLLING OFFICE NAME AND ADDRESS: David Taylor Naval Ship Research and Development Center (Code 1905), Bethesda, MD 20084 (11)	12. REPORT DATE: 19 December 1979
	13. NUMBER OF PAGES: 22
14. MONITORING AGENCY NAME & ADDRESS (if different from Controlling Office)	15. SECURITY CLASS. (of this report): UNCLASSIFIED
	15a. DECLASSIFICATION/DOWNGRADING SCHEDULE

16. DISTRIBUTION STATEMENT (of this Report)

Approved for public release; distribution unlimited.

(16) S0221AS

63562N

17. DISTRIBUTION STATEMENT (of the abstract entered in Block 20, if different from Report)

(17) S0221AS

18. SUPPLEMENTARY NOTES

19. KEY WORDS (Continue on reverse side if necessary and identify by block number)

Propagation Loss

Transmission Loss

20. ABSTRACT (Continue on reverse side if necessary and identify by block number)

A presentation on the transmission loss of a plane wave normally incident on multiple gratings of simply supported hollow bars emmersed in a fluid layer between two fluid half spaces was made at the 96th meeting of the Acoustical Society of America, held in Honolulu, Hawaii, during November 1978. This report documents the text and visual aids used in the presentation.

A

DD FORM 1 JAN 73 1473 EDITION OF 1 NOV 65 IS OBSOLETE
S/N 0102-014-6601

405 918

JOC

TABLE OF CONTENTS

LIST OF ILLUSTRATIONS

TRANSMISSION LOSS THROUGH CASCADED GRATINGS OF SIMPLY SUPPORTED HOLLOW BARS IN A FLUID LAYER

INTRODUCTION

Arrays of compliant tubes or compliant elements have been used extensively to provide directivity for transducer-reflector combinations, such as the Azores Fixed Acoustic Range (AFAR) system,[1] and as baffles for the reduction of self-noise. When the elements vibrate at a frequency corresponding to a structural resonance with net volume displacement, the dynamic compliance of the array increases significantly. By proper choice of the material constants for the elements, an array can be tuned to be an effective reflector at a desired frequency.

A simple approximate theory for the analysis of a plane wave normally incident on a planar grating of compliant tubing, together with experimental data, was first reported by Toulis[2] in 1957. In this work, there are expressions for the static and dynamic bulk modulus of a single element. A multiple scattering formulation for a generalized plane wave incident on an array of identical elliptically shaped shells with an arbitrary orientation in a planar grating was described by Brigham, Libuha, and Radlinski.[3] In that article, the effects of element orientation and spacing on the frequency of the array resonance and insertion loss bandwidth were investigated. Also reported were experimental measurements of insertion loss for multiple-layer gratings that were used to increase the bandwidth of reflectivity.

A waveguide approach to the analysis of a plane wave normally incident on a single infinite layer of simply supported compliant bars in an infinite fluid medium was attempted by Vovk, Grinchenko, and Kononuchenko.[4] The problem considered in this report is an extension of the work by Vovk et al. to include multiple planar gratings in a fluid layer of finite thickness between two fluid half spaces. The fluids can have different velocities and densities. We will investigate the broadband transmission loss that can be achieved through the use of at least two gratings in a fluid layer. In particular, bars with simply supported end conditions are considered.

MATHEMATICAL FORMULATION

DIFFERENTIAL EQUATIONS, BOUNDARY CONDITIONS, AND SOLUTIONS

In figure 1, a plane wave is shown to be normally incident on a double grating of compliant inclusions in a fluid layer. In an individual element, the two bars may have a different thickness, density, or Young's modulus and, therefore, can have two series of independent plate resonances. The connection between the simply supported plates is assumed to be rigid. In this example, both gratings have the same spacing, d, but multiple gratings of different spacings will also be considered. The waveguide solution is found by

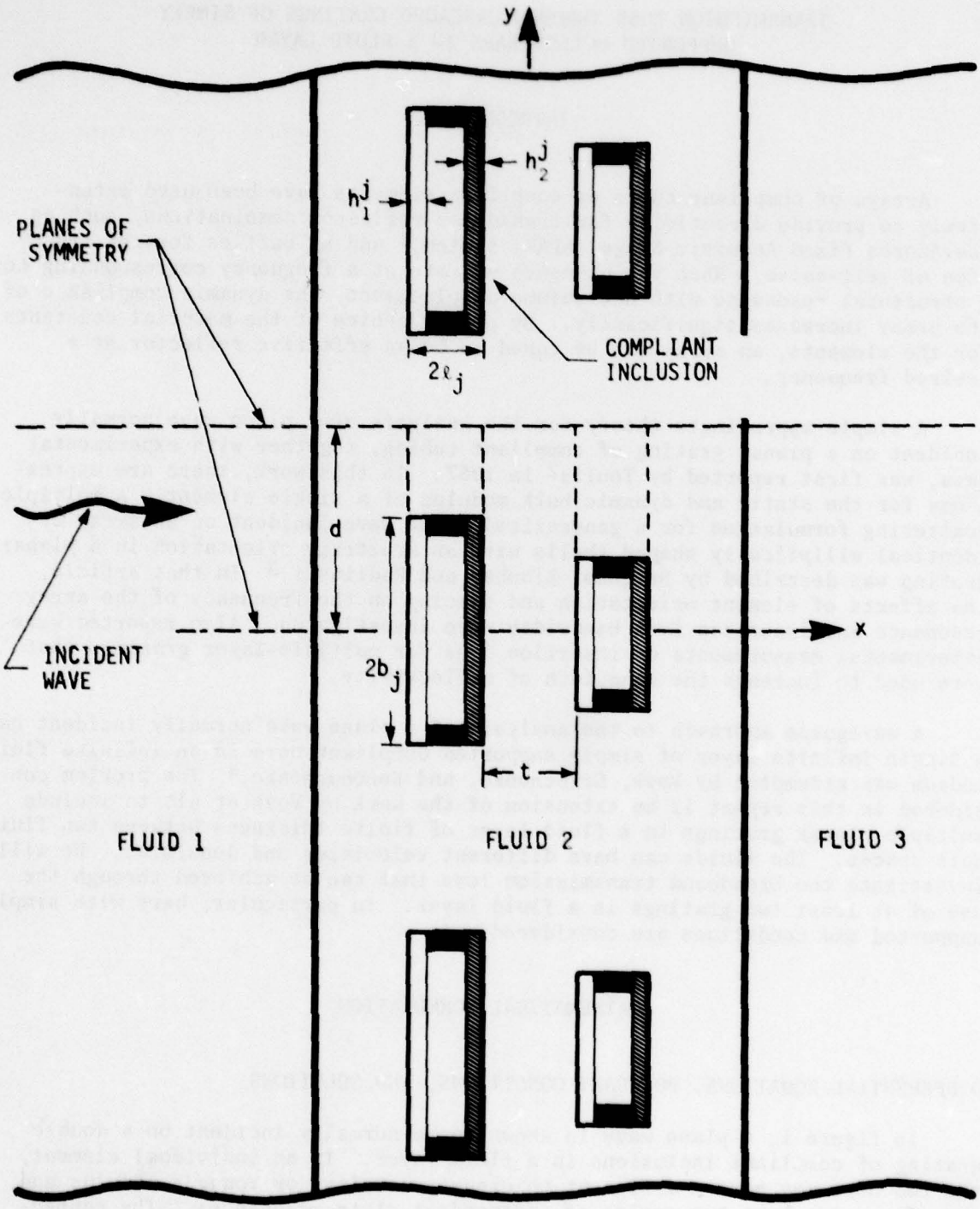

Figure 1. Double Grating of Simply Supported Elements in a Fluid Layer

satisfying the boundary conditions between the planes of symmetry shown in figure 1. The vertical lines (both solid and dashed) between the planes of symmetry delineate boundaries separating regions where the solutions to the wave equation vary.

The differential equations to be satisfied are the wave equation for the pressure in the fluid and the thin-plate equation, which is assumed to govern the motion of the bars. The wave equation for the pressure in the fluid is given by

$$\nabla^2 P_i + k_i^2 P_i = 0 \ , \tag{1}$$

where k_i is the wavenumber of the i-th fluid and P_i is the pressure in the i-th fluid. The thin-plate equation for compliant plate motion of the inclusions is given in the form

$$D_q \frac{d^4 W_q(y)}{dy^4} - \mu_q \omega^2 W_q(y) = P_i \ , \tag{2}$$

where

D_q is the flexural rigidity of the q-th plate,

μ_q is the mass per unit area of the plate,

ω is the circular frequency, and

W_q is the displacement of the plate.

The boundary conditions imposed at the fluid interfaces, symmetry planes, and tube surfaces are given by the following. At the fluid interfaces, the two boundary conditions to be satisfied are the continuity of pressure

$$P_i = P_j \tag{3}$$

and continuity of normal velocity

$$\frac{1}{i\omega\rho_i^f} \frac{\partial P_i}{\partial x} = \frac{1}{i\omega\rho_j^f} \frac{\partial P_j}{\partial x} \tag{4}$$

between the adjacent i-th and j-th regions, and ρ^f is the density of the fluid. The condition on the velocity normal to the symmetry planes is

$$\frac{\partial P_i}{\partial y} = 0 \ ; \ |y| = d \ , \ |x| < \infty \ . \tag{5}$$

At the tube surfaces, the three boundary conditions to be met are for (1) the nondeformable supports,

$$\frac{\partial P_i}{\partial y} = 0 \; ; \; |y| = b_j \; , \; -\ell_j + x_j < x < x_j + \ell_j \; , \tag{6}$$

where x_j is the x coordinate of the center of the j-th grating and ℓ_j is the half width of the inclusion; (2) the continuity of normal displacement at the flexible plates,

$$\frac{1}{\omega^2 \rho_i^f} \frac{\partial P_i}{\partial x} = W_q(y) \; ; \; |y| \leq b_j \; , \; x = \pm \ell_j + x_j \; ; \tag{7}$$

and (3) the simply supported condition,

$$W_q(y) = \frac{d^2 W_q(y)}{dy^2} = 0 \; ; \; |y| = b_j \; , \tag{8}$$

at

$$x = \pm \ell_j + x_j \; .$$

The solution for the total pressure in the half space of fluid 1 is the sum of the incident plane wave and an infinite series of reflected waves, as indicated by the expression

$$P_1 = e^{ik_1 x} + \sum_{n=o}^{\infty} R_n \exp\left(-ik_n^o (x - x_0)\right) \cos \alpha_n y$$
$$k_n^o = \sqrt{k_1^2 - \alpha_n^2} \; ; \; \alpha_n = \frac{n\pi}{d} \; , \tag{9}$$

where

k_1 is the wavenumber in fluid 1,

x_o is the x coordinate of the boundary between fluid 1 and fluid 2, and

R_n is a reflection coefficient to be determined.

When $k_1^2 > \alpha_n^2$, this wave propagates away from the grating. However, if $k_1^2 < \alpha_n^2$, the wave propagates parallel to the y axis and decays exponentially in the x direction away from the grating. Such a wave is often referred to as an evanescent wave. The grazing modes are defined by $k_1^2 = \alpha_n^2$. In fluid layer 2 with inclusions, the solution, in each of the j regions defined by the vertical lines in figure 1, consists of an infinite series of waves of the form

$$P_2^{(j)} = \sum_{m=0}^{\infty} \left\{ A_m^{(j)} \cos k_m^{(j)} \left(x - x_j^0 \right) + B_m^{(j)} \sin k_m^{(j)} \left(x - x_j^0 \right) \right\} \cos \alpha_{m_j} \left(y - c_i \right) , \tag{10}$$

$$k_m^{(j)} = \sqrt{k_2^2 - \alpha_{m_j}^2} , \quad \alpha_{m_j} = \frac{m\pi}{d - c_j} .$$

Here c_j is a constant determined by satisfying either equation (5) and/or equation (6), as appropriate, for region j of the fluid layer. The factor k_2 is the wavenumber in fluid 2, x_j is the x coordinate at the center of the j-th region, and $A_m^{(j)}$ and $B_m^{(j)}$ are unknowns in region j of the fluid layer. The transmitted pressure waves in fluid 3 are of particular importance in this report and are given by the expression

$$P_3 = \sum_{n=0}^{\infty} T_n \exp\left[ik_n' \left(x - x_m \right) \right] \cos \alpha_n y , \tag{11}$$

where

$$k_n' = \sqrt{(k_3)^2 - \alpha_n^2} ,$$

k_3 is the wavenumber in fluid 3,

x_m is the x coordinate of the boundary between fluids 2 and 3, and

T_n is an unknown transmission coefficient.

For the compliant elements, a normal-mode solution to the plate equation is given by the displacement distribution

$$W_q(y) = \sum_{s=0}^{\infty} W_s^{(q)} \cos \alpha_s^q y, \quad \alpha_s^q = \frac{(2s + 1)\pi}{2b_q} , \tag{12}$$

where $W_s^{(q)}$ are unknown amplitudes determined from the boundary conditions. If the above expression for the displacement is substituted into the homogeneous plate equation, the natural frequencies of the plates in vacuum are seen to be

$$f_s^{(q)} = \frac{h_q}{2\pi} \left[\frac{\pi(2s + 1)}{2b_q} \right]^2 \sqrt{\frac{E_j}{12\rho_q \left(1 - \sigma_q^2 \right)}} , \tag{13}$$

where ρ_q, E_q, σ_q, $2b_q$, and h_q are the density, Young's modulus, Poisson ratio, length, and thickness of the q-th plate.

SYSTEM OF LINEAR ALGEBRAIC EQUATIONS

The unknown pressure distributions and displacement amplitudes of the plate motion are found by satisfying the boundary conditions between the various regions. For the configuration shown in figure 1, the set of equations arising from the matching conditions is easily transformed on the basis of completeness and orthogonality into an infinite system of linear algebraic equations such that by satisfying equations (3) and (4) at the two boundaries $\left(x = x_0;\ x_M\right)$ that separate the semi-infinite media by a layer of M regions, we obtain

$$\left[A_n^{(1)} \cos k_n\left(x_0 - x_1^0\right) + B_n^{(1)} \sin k_n\left(x_0 - x_1^0\right) - R_n\right]N_n = e^{ik_0 x_0}\delta_n$$

$$\left[A_n^{(M)} \cos k_n\left(x_M - x_M^0\right) + B_n^{(M)} \sin k_n\left(x_M - x_M^0\right) - T_n\right]N_n = 0$$

$$\left\{\frac{k_n}{\rho_2^f}\left[-A_n^{(1)} \sin k_n\left(x_0 - x_1^0\right) + B_n^{(1)} \cos k_n\left(x_0 - x_1^0\right)\right] + \frac{ik_n^0 R_n}{\rho_1^f}\right\}N_n = \frac{ik_0}{\rho_0} e^{ik_0 x_0}\delta_n \tag{14}$$

$$\left\{\frac{k_n}{\rho_2^f}\left[-A_n^{(M)} \sin k_n\left(x_M - x_M^0\right) + B_n^{(M)} \cos k_n\left(x_M - x_M^0\right)\right] - \frac{ik_n' T_n}{\rho_3^f}\right\}N_n = 0$$

and by satisfying equations (2) and (7) at the M - 1 regional interfaces determined by the q-th plate position $\left(x = x_q,\ 0 < y < b_j\right)$ and satisfying equations (2) and (3) at the fluid boundary $\left(x = x_q,\ b_j < y < d\right)$, which separates the i-th region to the front of the plate from the fluid interstice above the inclusion (region j), we also obtain equations of the form

$$\frac{\rho_q h_q b_q}{2}\left\{\left[\omega_s^{(q)}\right]^2 - \omega^2\right\}W_s^{(q)} = \operatorname{sgn}(P)\sum_{n=o}^{\infty}\left[A_n^{(i)} \cos k_n\left(x_q - x_i^0\right) + B_n^{(i)} \sin k_n\left(x_q - x_i^0\right)\right]N_{ns}$$

$$\left[A_m^{(j)} \cos k_m^{(j)}\left(x_q - x_j^0\right) + B_m^{(j)} \sin k_m^{(j)}\left(x_q - x_j^0\right)\right]N_m \tag{15}$$

$$= \sum_{n=0}^{\infty}\left[A_n^{(i)} \cos k_n\left(x_q - x_i^0\right) + B_n^{(i)} \sin k_n^{(j)}\left(x_q - x_i^0\right)\right]N_{nm}$$

$$k_n\left[-A_n^{(i)} \sin k_n\left(x_q - x_i^0\right) + B_n^{(i)} \cos k_n\left(x_q - x_i^0\right)\right] N_n$$

$$= \sum_{m=0}^{\infty} k_n^{(j)}\left[A_m^{(j)} \sin k_m^{(j)}\left(x_q - x_j^0\right) + B_m^{(j)} \cos k_m^{(j)}\left(x_q - x_j^0\right)\right] N_{nm}$$

$$+ \omega^2 \rho_2^f \sum_{s=0}^{\infty} W_s^{(q)} N_{ns} \ ,$$

where the following notation is used

$$N_{nm} = \begin{cases} d - b; \ n = m = 0 \ , \\ \dfrac{d - b}{2}\left\{\cos\left(\dfrac{m\pi}{d - b}\right) b - \dfrac{1}{m\pi} \sin\left(\dfrac{m\pi}{d - b}\right) b\right\} \ ; \ n(d - b) = md \neq 0 \ , \\ \dfrac{n \sin \dfrac{n\pi b}{d}}{\pi d\left[\left(\dfrac{m}{d - b}\right)^2 - \left(\dfrac{n}{d}\right)^2\right]} \ ; \ n(d - b) \neq md \ , \end{cases}$$

$$N_n = \begin{cases} d \ ; \ n = 0 \ , \\ d/2 \ ; \ n \neq 0 \ , \end{cases}$$

$$N_m = \begin{cases} d - b \ ; \ m = 0 \ , \\ (d - b)/2 \ ; \ m \neq 0 \ , \end{cases}$$

$$N_{ns} = \begin{cases} 2h_j(-1)^s/\pi(2s + 1) \ ; \ n = 0 \ , \\ b_j/2 \ ; \ 2nb_j = d(2s + 1) \neq 0 \ , \\ \dfrac{(-1)^{s+1}(2s + 1) \cos \dfrac{n\pi b_j}{d}}{2\pi b_j\left\{\left(\dfrac{n}{d}\right)^2 - \left[\dfrac{(2s + 1)}{2b_j}\right]^2\right\}} \ ; \ 2nb_j \neq d(2s + 1) \ , \end{cases}$$

$$\delta_n = \begin{cases} d \ ; \ n = 0 \ , \\ 0 \ ; \ n \neq 0 \ , \end{cases}$$

$$\omega_s^{(q)} = 2\pi f_s^{(q)} \ ,$$

$$k_m^{(j)} = \sqrt{k_2^2 - \alpha_{m_j}^2} \ ; \ \alpha_{m_j} = \frac{m\pi}{d - b_j}$$

$$k_n = \sqrt{k_2^2 - \alpha_n^2} \ ; \ \alpha_n = \frac{n\pi}{d}$$

Here, sgn (P) is the sign of the pressure on the plate determined by the chosen sign convention. The convention chosen in the work of Vovk et al.[4] does not appear to satisfy the condition that a plane wave incident from the

left side of the layer results in the same insertion loss as a plane wave incident from the right side if the layer is unsymmetric and is reversed in position.

For multiple gratings with different grating spacings, the above formulation is extended to include configurations in which planes of symmetry are common to all the individual gratings. The boundary conditions are then satisfied between these planes of symmetry. The complexity of the resulting system of equations increases somewhat because of the increased number of compliant elements within the symmetry planes.

MODEL CALCULATIONS

Using the analytical techniques described earlier, one can investigate the interaction between gratings, transmission resonances of a fluid layer with inclusions, and the effects of changing material constants within the gratings. In particular, it is often desired to maximize the transmission loss bandwidth by using more than one grating of compliant elements. Comparisons with perfectly soft or perfectly rigid inclusions are often instructive. The calculations presented here are for the maximum grating spacing being less than a wavelength in fluid layer 3. The transmission coefficient is then completely determined by the value of the unknown coefficient T_0 because all waves of higher order are evanescent. Calculations of T_0 from truncated series determined by satisfying the boundary conditions were shown to converge by retaining four to five values of each unknown in the linear system of equations.

MULTIPLE GRATINGS WITH IDENTICAL GRATING SPACING

Several examples will be presented in this section that analyze the dependence of the transmission loss on frequency for several different parameters.

Comparison of the Transmission Loss for Single and Double Gratings

An example of the increased transmission loss that results from a double grating is shown in figure 2. The transmission loss is plotted versus frequency normalized to the frequency of the first bending resonance of the plates in vacuum (f_1). In this example, and unless otherwise stated, water is assumed for all three fluids. The distance between the center lines of the two gratings is $0.0625\lambda_1$. A structural damping factor of 0.1 was assumed for the plates. When the transmission loss has a large value, most of the energy of the incident plane wave is reflected by the gratings and the magnitude of the velocity of the back plate is small relative to the plate velocity on the incident wave side. Note that both the maximum transmission loss and the bandwidth are increased with the use of a second identical layer. In most uses of compliant elements, the experimental values of transmission loss are

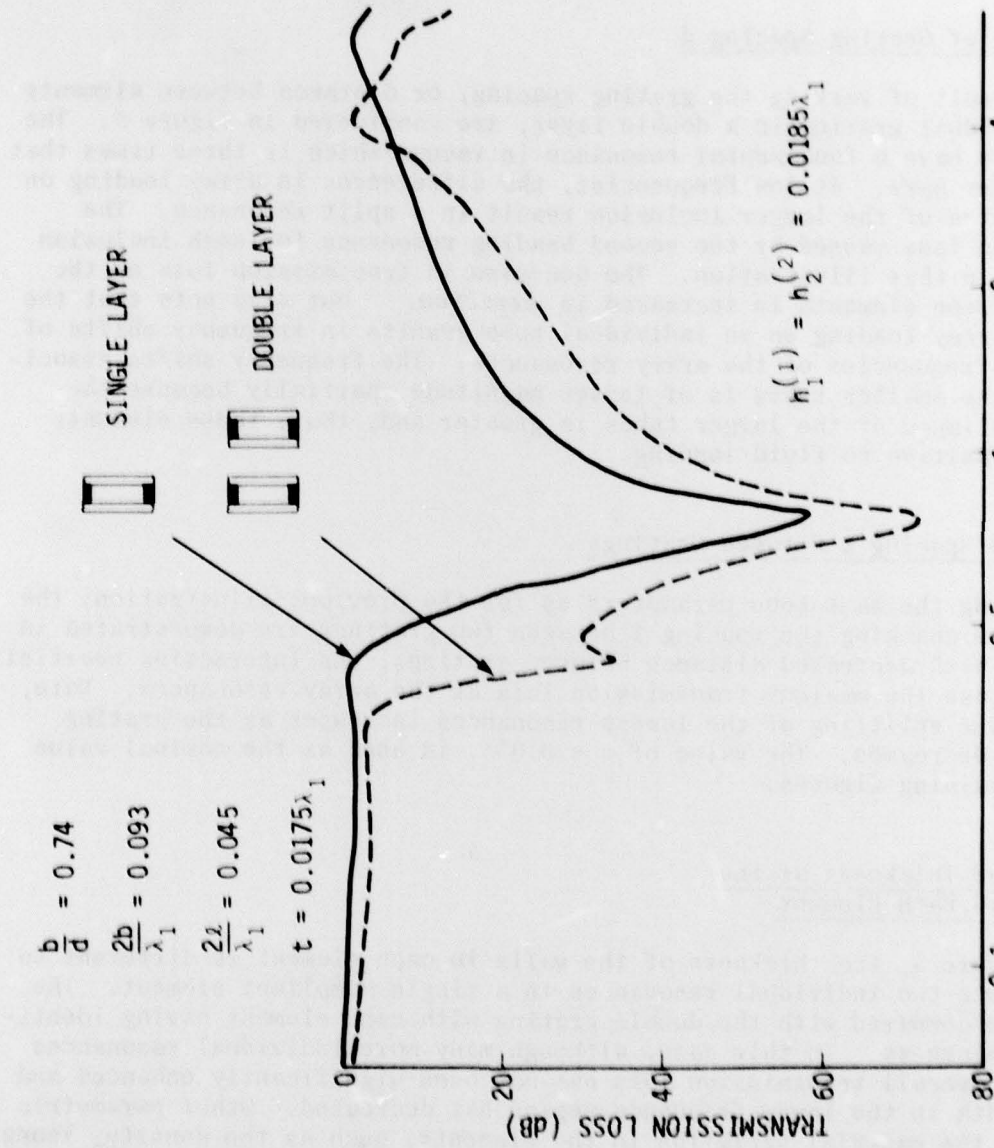

Figure 2. Comparison of Single and Double Gratings of Equal-Sized Elements

reduced by rigid body motion and edge diffraction, neither of which is considered in this analysis. The elastic plates are considered to be identical and are constructed of lexan plastic ($\rho = 1.18 \times 10^3$ kg/m^3, $E = 2.38 \times 10^9$ n/m^2, $\sigma = 0.375$, $h_1^{(1)} = h_2^{(1)} = 0.0185\lambda_1$). The radiation loading on the two inner plates in the double layer causes the secondary maximum in transmission loss at $f = 0.4f_1$.

The Effects of Grating Spacing d

The result of varying the grating spacing, or distance between elements in an individual grating in a double layer, are considered in figure 3. The smaller bars have a fundamental resonance in vacuum which is three times that of the larger bars. At low frequencies, the differences in array loading on the two plates of the larger inclusion result in a split resonance. The transmission loss caused by the second bending resonance for each inclusion is evident in this illustration. The decrease in transmission loss as the spacing between elements is increased is expected, but also note that the change in array loading on an individual tube results in frequency shifts of the center frequencies of the array resonances. The frequency shifts associated with the smaller tubes is of lesser magnitude, partially because the static compliance of the larger tubes is greater and, thus, these elements are more sensitive to fluid loading.

Varying the Spacing t Between Gratings

By using the same tube parameters as for the previous illustration, the results from changing the spacing t between two gratings are demonstrated in figure 4. With decreased distance between gratings, the interacting nearfield terms decrease the maximum transmission loss at the array resonances. Note, also, how the splitting of the lowest resonances increases as the grating separation decreases. The value of $t = 0.03\lambda_1$ is used as the nominal value for the remaining figures.

Changing the Thickness of the Two Walls in Each Element

In figure 5, the thickness of the walls in each element is different so as to produce two individual resonances in a single compliant element. The results are compared with the double grating with each element having identical wall thickness. In this case, although many more individual resonances occur, the overall transmission loss has not been significantly enhanced and the bandwidth in the lower frequency region has decreased. Other parametric studies of the material variation in the elements, such as the density, Young's modulus, and Poisson's ratio may be made to broaden the bandwidth of transmission loss. In this example the variation in the frequencies is directly proportional to the change in thickness.

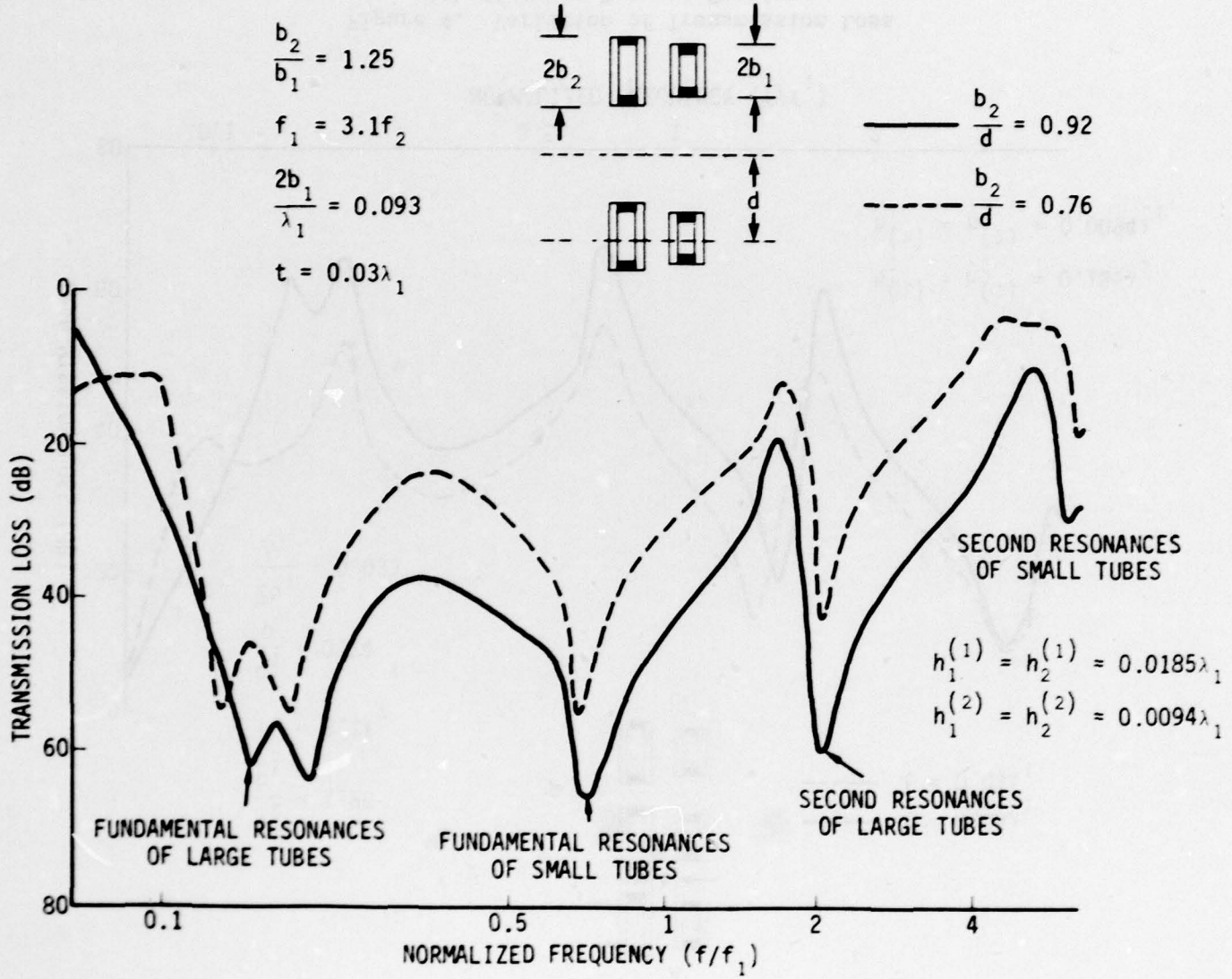

Figure 3. Effects of Grating Spacing

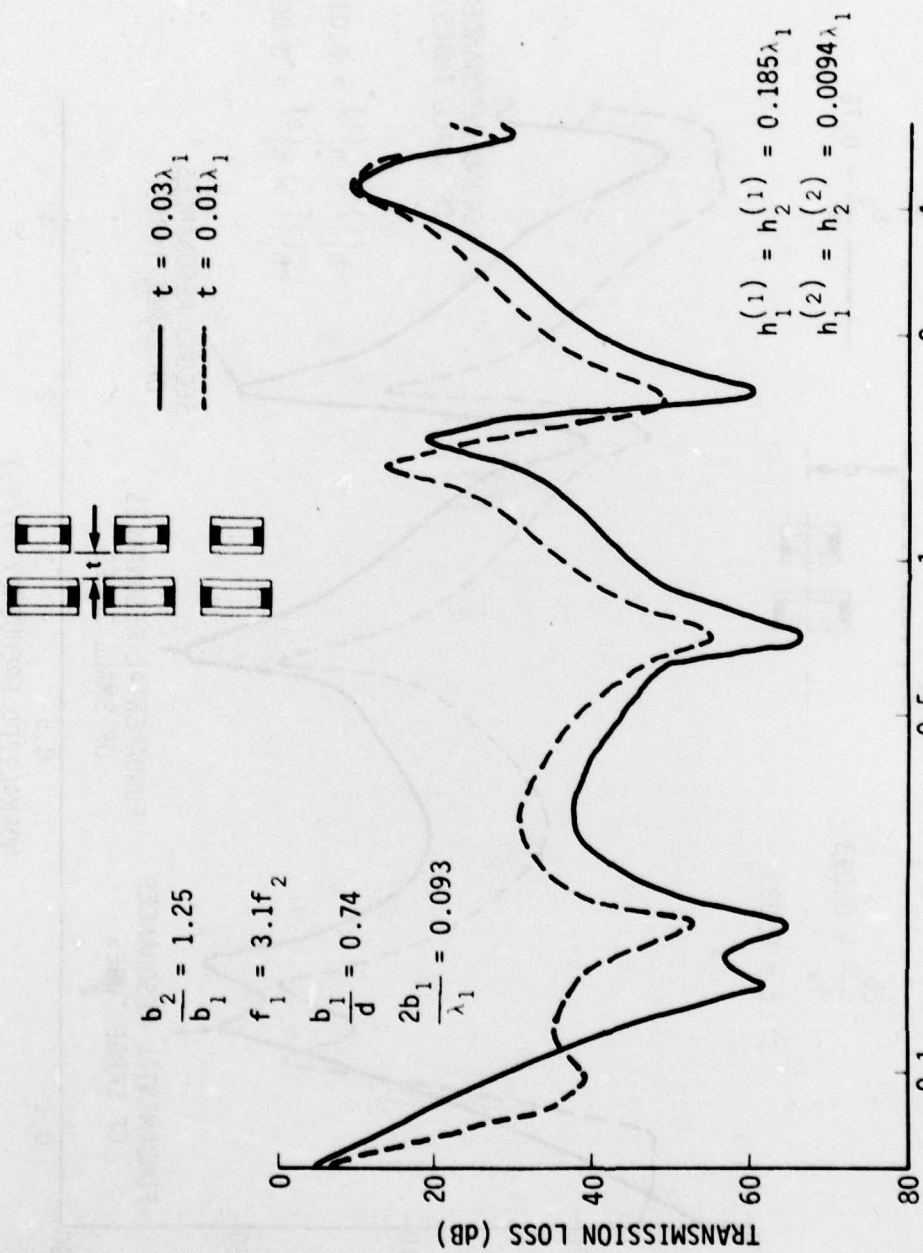

Figure 4. Variation of Transmission Loss With Distance Between Gratings

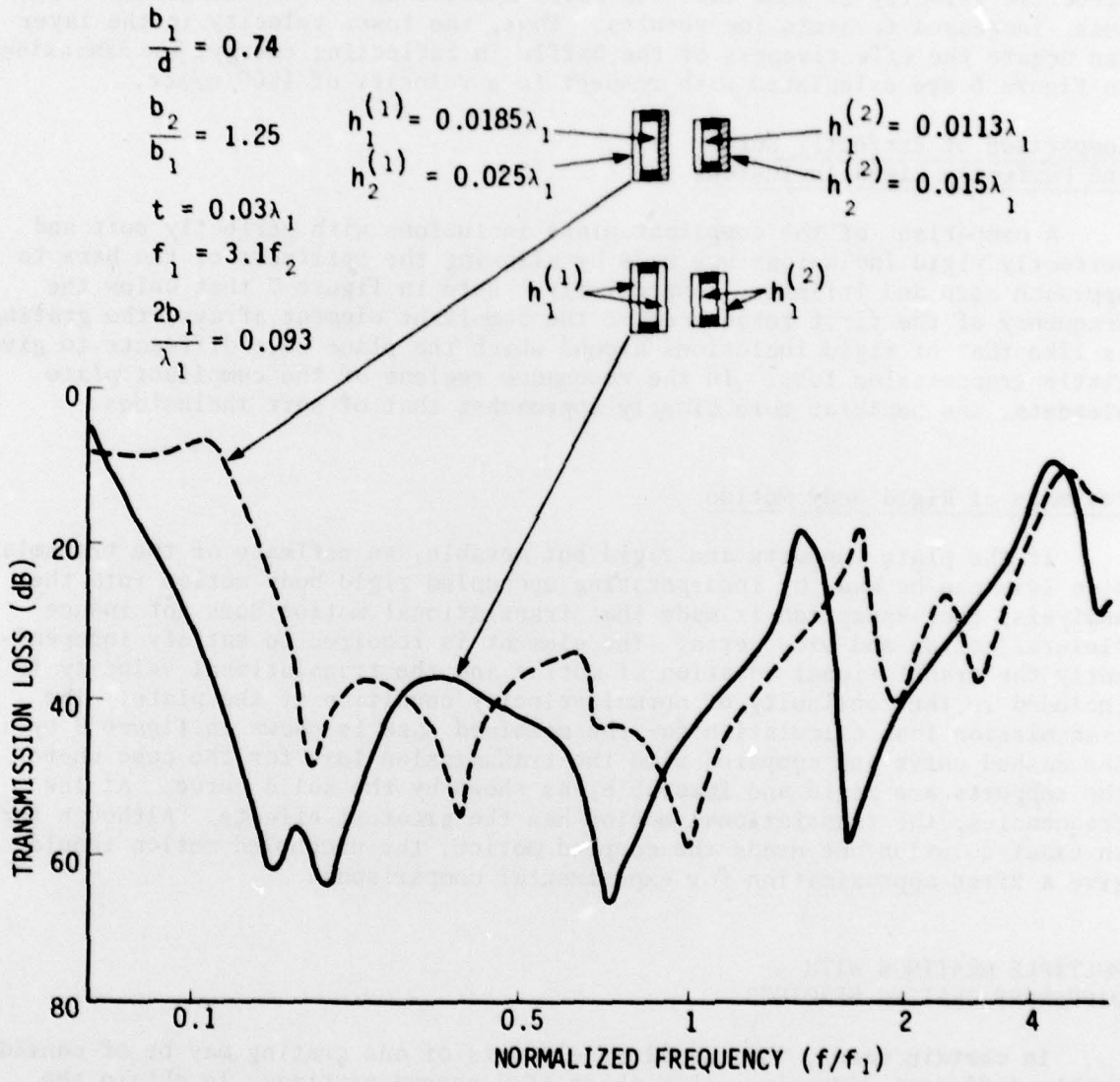

Figure 5. Comparison of Transmission Losses With Plate Thicknesses Different in a Single Inclusion

Variation of the Velocity of the Fluid Layer

The effects on transmission loss from varying the velocity of the fluid layer are shown in figure 6. For a fluid-layer velocity of about 1500 m/s, shown by the solid curve, only the four distinct array resonances are evident. Now, as the velocity of the layer is decreased to about 150 m/s, as shown by the dashed curve, transmission resonances appear at the higher frequencies. The transmission resonances are associated with layer thickness. When the effective velocity is such that the layer approaches 0.5 wavelength in thickness, increased transmission results. Thus, the lower velocity in the layer can negate the effectiveness of the baffle in reflecting energy. The dimensions in figure 6 are calculated with respect to a velocity of 1500 m/sec.

Comparison of Perfectly Soft and Perfectly Rigid Inclusions

A comparison of the compliant plate inclusions with perfectly soft and perfectly rigid inclusions was made by allowing the stiffness of the bars to approach zero and infinity, respectively. Note in figure 7 that below the frequency of the first resonances of the compliant element arrays, the grating is like that of rigid inclusions around which the plane wave diffracts to give little transmission loss. In the resonance regions of the compliant plate elements, the behavior more closely approaches that of soft inclusions.

Estimate of Rigid Body Motion

If the plate supports are rigid but movable, an estimate of the transmission loss can be made by incorporating uncoupled rigid body motion into the analysis; the assumption is made that translational motion does not induce flexural motion and vice versa. The element is required to satisfy independently the translational equation of motion and the translational velocity is included in the continuity of normal velocity condition at the plate. The transmission loss calculation for the combined case is shown in figure 8 by the dashed curve and compared with the transmission loss for the case where the supports are rigid and immovable, as shown by the solid curve. At low frequencies, the translational motion has the greatest effects. Although for an exact solution one needs the coupled motion, the uncoupled motion should give a first approximation for experimental comparisons.

MULTIPLE GRATINGS WITH DIFFERENT GRATING SPACINGS

In certain cases, the compliant elements of one grating may be of considerably different dimensions than those of a second grating. To obtain the maximum transmission loss, a dense packing of both gratings may be necessary. In this case, more of the smaller elements will be used for a given grating length.

For the cases considered in this section, the larger tube is the same as was used earlier and the smaller tube is half the width but has three times the resonance frequency in air of the larger tube. A double grating with the

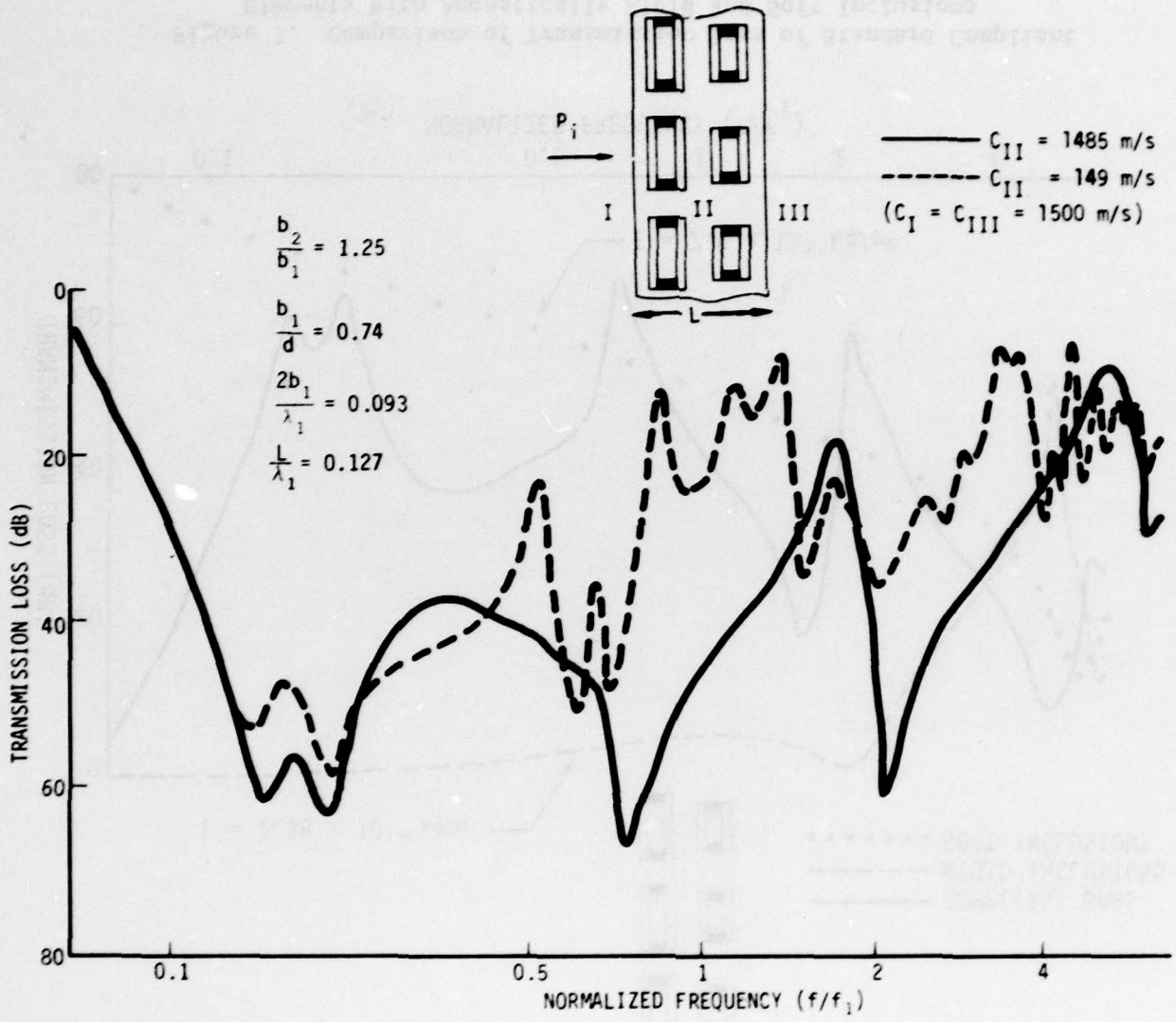

Figure 6. Variation of Transmission Loss With Velocity of Sound in the Fluid Layer

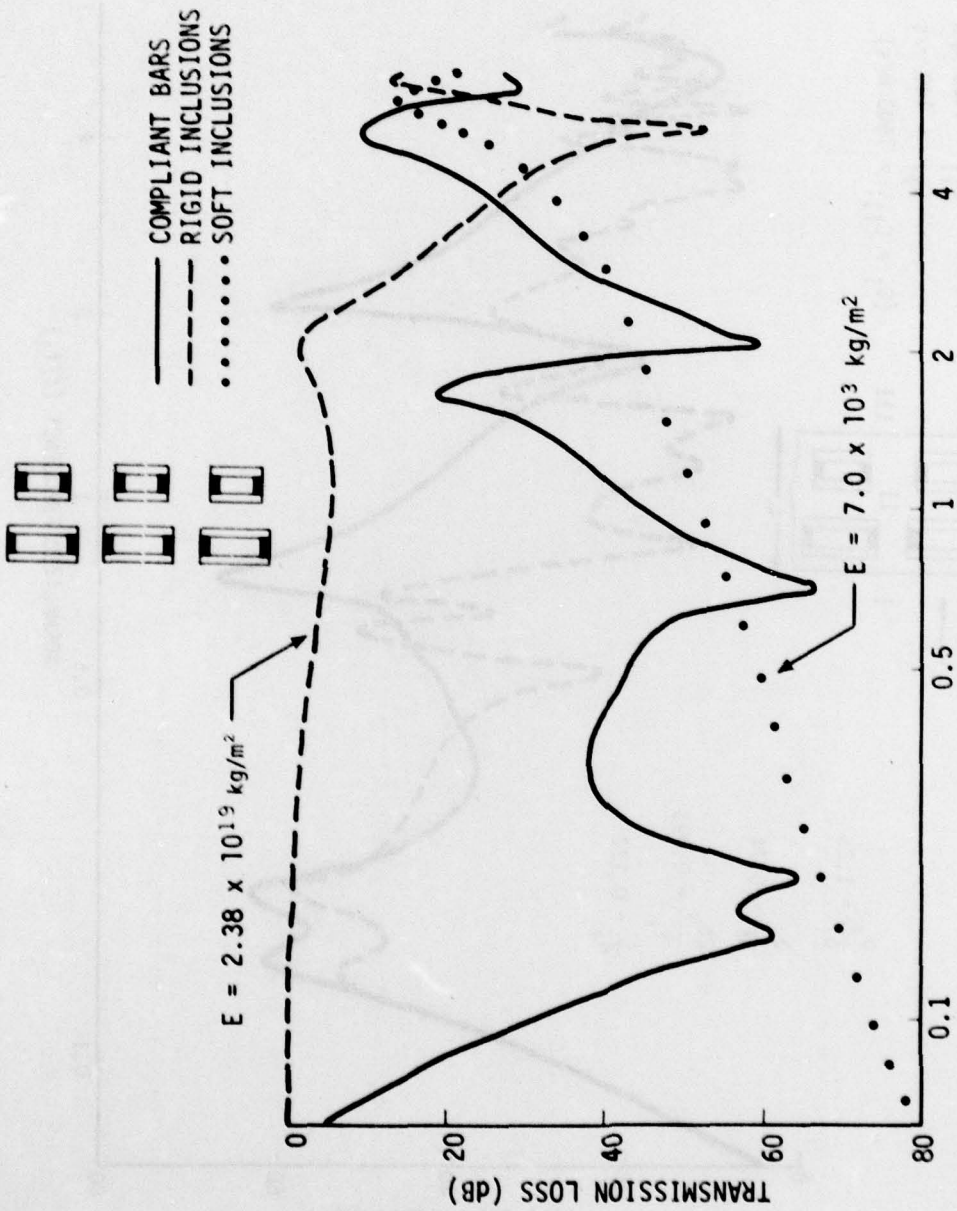

Figure 7. Comparison of Transmission Loss of Standard Compliant Elements With Acoustically Rigid and Soft Inclusions

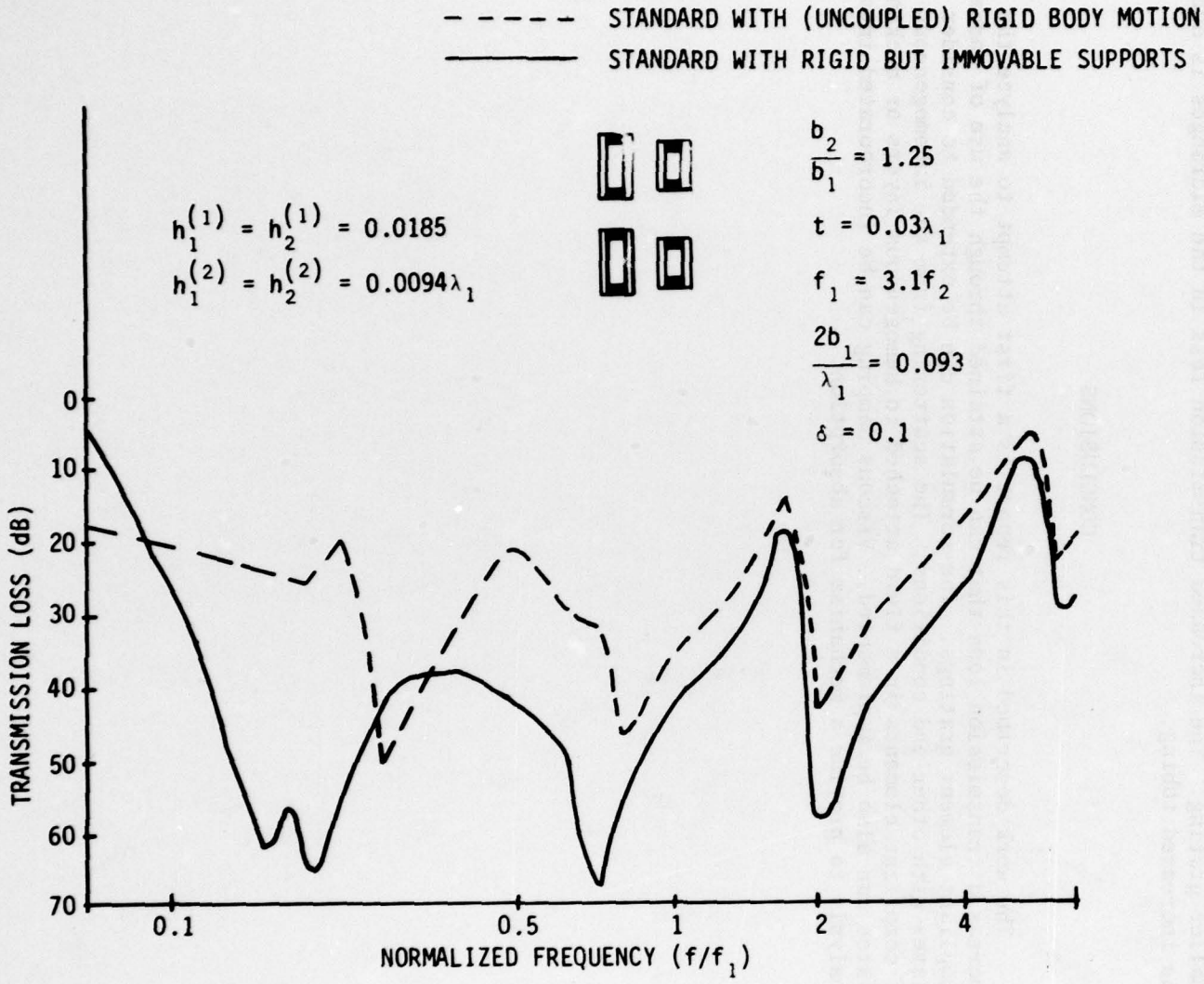

Figure 8. Estimate of Transmission Loss for Compliant Plates With Rigid But Movable Supports

same grating spacing is compared in figure 9 with a second grating having twice the number of tubes. Several differences are evident in the two cases. With the denser second layer, the resulting array loading causes a wide separation of the fundamental transmission loss resonances of the larger tube. The second transmission loss resonance is higher than for the widespread smaller grating. The increased transmission loss in the midranges is due to the increased tubing.

CONCLUSIONS

The work described in this report is a first attempt to analyze the increased transmission loss that can be attained through the use of cascaded compliant element gratings. The formulation can be extended to consider plates with other end conditions. The scattering from the inhomogeneous layer of compliant elements in a fluid attached to homogeneous layers or backing plates can also be implemented. Viscous damping can be incorporated into the analysis to provide a mechanism for absorption.

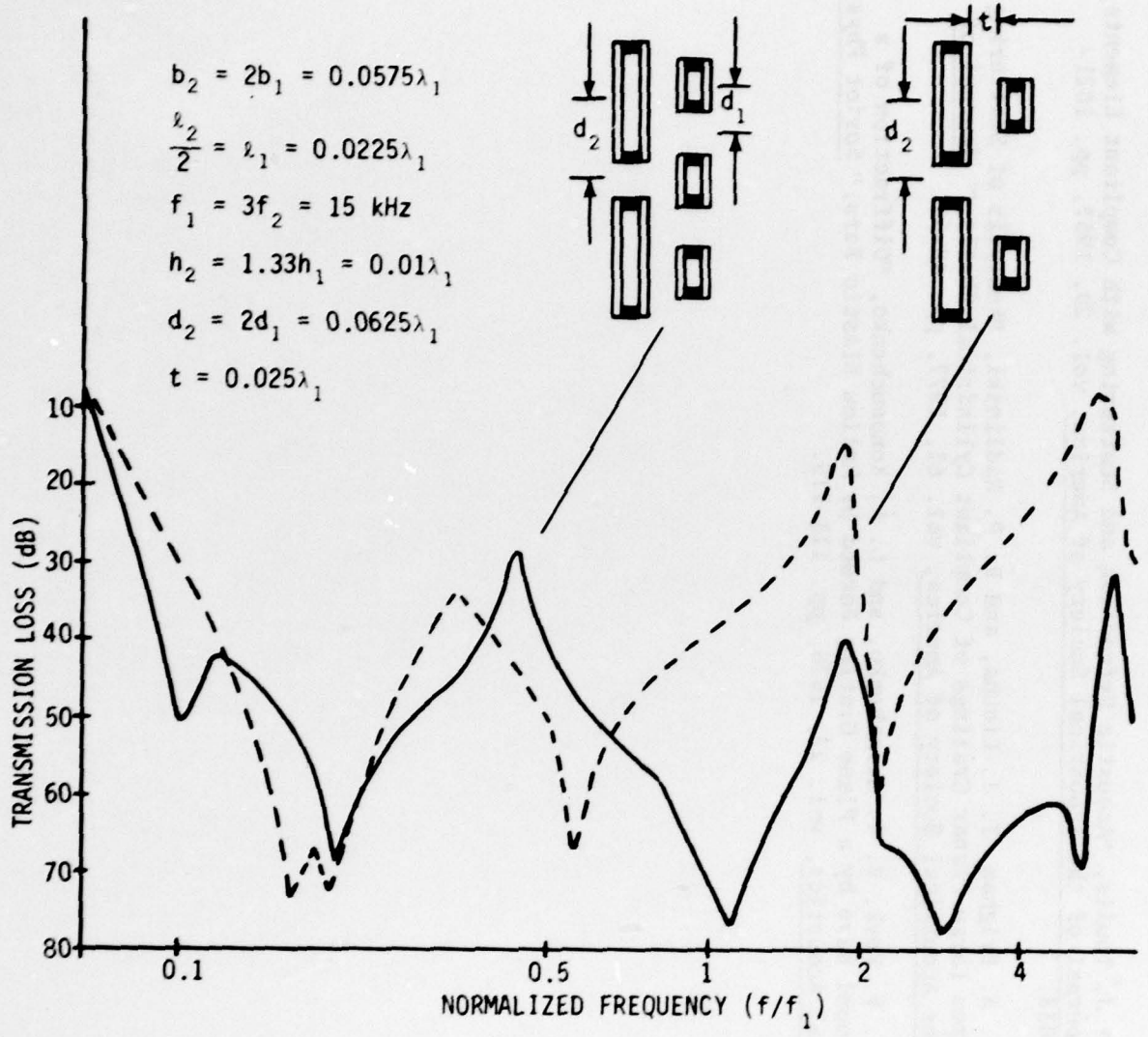

Figure 9. Comparison of Transmission Loss of Double Gratings With Different Grating Spacings

REFERENCES

1. A. W. Ellinthorpe, The Azores Range, NUSC Technical Document 4551, Naval Underwater Systems Center, New London, CT, April 1973.

2. W. J. Toulis, "Acoustic Refraction and Scattering with Compliant Elements," Journal of the Acoustical Society of America, vol. 29, 1957, pp. 1021-1033.

3. G. A. Brigham, J. J. Libuha, and R. P. Radlinski, "Analysis of Scattering from Large Planar Gratings of Compliant Cylindrical Shells," Journal of the Acoustical Society of America, vol. 61, 1977, pp. 48-59.

4. I. V. Vovk, V. T. Grinchenko, and L. A. Kononuchenko, "Diffraction of a Sound Wave by a Plane Grating Formed by Hollow Elastic Bars," Soviet Physical Acoustics, vol. 22, 1976, pp. 113-115.

INITIAL DISTRIBUTION LIST

Addressee	No. of Copies
ASN (RE&S) (D. E. Mann)	1
OUSDR&E (Research & Advanced Technology (W. J. Perry)	2
Deputy USDR&E (Res & Adv Tech) (R. M. Davis)	1
Deputy USDR&E (Dir Elect & Phys Sc) (L. Wiseberg)	1
OASN, Spec Dep for Adv Concept (Dr. D. Hyde)	1
OASN, Dep Assist Secretary (Systems) (M. G. Cann)	1
OASN, Dep Assist Secretary (Res & Adv Tech) (Dr. R. Hoglund)	1
ONR, ONR-100, -220, -102, -212, -222, -230	6
CNO, OP-02, -090, -098	3
CNM, MAT-00, -08T, -08T2, -08T1, -08T12, -08T24, ASW-23,	7
CNM, Special Projects Office (PM-2) Trident	1
DWTNSRDC ANNA	1
DWTNSRDC CARD (Mel Rumerman, Code 1965, Wayne T. Reader, Code 1900)	3
NRL (L. Flax)	2
NRL, USRD	1
NORDA (Dr. R. Goodman, 110)	1
USOC, Code 241, 240	2
NAVOCEANO, Code 02	1
NAVELECSYSCOM, ELEX 03, 320 (J. C. Bertrand)	2
NAVSEASYSCOM, SEA-000,-003,-03, -05H (C. C. Taylor)(2), -06D, -06R, -61, -61R, -62R, -63R(2), -63R-1, -631X, -631Y, -6334, PMS-402, SEA-92, -92R, -395, -396, -93, 996	23
NOSC (P. Barakos)	3
DWTNSRDC(Rippeon, Code 1908, Goodman)	2
NAVCOASTSYSLAB	1
NAVSURFWPNCEN (G. C. Gaunard, W. Madagowski)	2
NUWES	1
NOSC, Naval Ocean Systems Center (J. Cummings)	1
FLTASWTRACENLANT	5
NAVPGSCOL	1
Ohio State University, Dept. of Engr. Mech., Boyd Lab., Columbus,OH (Dr. V. J. Varadan)	1
Analysis and Technology, N. Stonington, CT (Dr. Murray Simon)	1
ARL/PENN STATE, STATE COLLEGE (Jan Holland, S. Hayek)	2
DTIC	12
DARPA (T. Kooij)	1
NOAA/ERL	1
WOODS HOLE OCEANOGRAPHIC INSTITUTION	1
BOLT, BERANEK & NEWMAN INC., Cambridge, MA (F. Berkman, E. Kerwin)	2
ENGINEERING SOCIETIES LIBRARY, UNITED ENGRING CTR	1
ARL, UNIV OF TEXAS (J. Willman)	1
MARINE PHYSICAL LAB, SCRIPPS	1
CAMBRIDGE ACOUSTICAL ASSOCIATES, 54 Rindge Ave., Cambridge, MA (Joel Garrelick)	1
CAMBRIDGE COLLABORATIVE, Cambridge, MA (Dr. James Moore)	1
AMERICAN UNIVERSITY, Physics Dept., Washington, DC (Dr. R. V. Waterhouse)	1
SACLANT RESEARCH CENTRE (Benjamin Helm)	1